

Joint Noncoherent Detection and Channel Decoding for UWB Impulse Radio by Belief Propagation

Taotao Wang, *Student Member, IEEE*, Tiejun Lv, *Senior Member, IEEE*, Hui Gao, *Member, IEEE*, Shengli Zhang, *Member, IEEE*

Abstract—This paper proposes a belief propagation (BP) algorithm based joint noncoherent detection and channel decoding scheme for ultra-wideband impulse radio (UWB-IR) systems. Multiple symbol differential detection (MSDD) can enhance the performance of noncoherent differential UWB-IR systems. Channel codes are usually employed to protect wireless transmissions over various impairments. Thus, it is naturally required to incorporate channel decoding with MSDD for noncoherent UWB-IR systems. In this paper, we propose a new auto-correlation receiver (AcR) architecture to sample the received UWB-IR signal. The statistical model of the signal samples has a trellis structure. Then, we apply BP algorithm on this trellis to derive a soft-in soft-out (SISO) MSDD, which is easy to be incorporated with SISO channel decoding. Simulation results indicate the advantage of the proposed joint noncoherent detection and channel decoding scheme.

Index Terms—Ultra-wideband (UWB), multiple symbol differential detection (MSDD), channel decoding, belief propagation (BP).

I. INTRODUCTION

ULTRA-wideband impulse radio (UWB-IR) is served as a promising candidate for location-aware indoor communications, wireless sensor networks and wireless personal area networks. UWB-IR has earned significant attentions in both academia and industry [1]. However, the implementation of optimal coherent receiver for UWB-IR systems faces many challenges. UWB channels usually contain hundreds of multipath, due to the rich scattering indoor environments. The optimal coherent receiver required to capture multipath energy is the famous Rake receiver [2]. Since the UWB channel is characterized by the dense multipath, we need a large number of Rake fingers to capture a significant part of the signal energy [3]. The implementation of so many Rake fingers and the associated channel estimation on the corresponding multipaths involve intensive complexities [4]. Moreover, such Rake receiver is very sensitive to timing-jitter [5]. These challenges make it difficult and costly to realize the optimal coherent receiver for UWB-IR systems.

In order to bypass these challenges, the suboptimal noncoherent receivers are proposed to obviate the complicated treatments on UWB channels [6]. The typical noncoherent UWB-IR schemes are differential [7] and transmitted-reference [8] UWB-IR systems, both deployed with analog autocorrelation receiver (AcR) that does not require Rake receiver and explicit channel estimation. Due to their good performance-complexity tradeoff, noncoherent receivers now are more popularly used in UWB-IR systems. However, they suffer from performance degradations compared with coherent receivers.

Multiple symbol differential detection (MSDD) is an effective means of improving performance for noncoherent differential UWB-IR systems. The theoretical framework of MSDD is the maximum-likelihood (ML) sequence detection, which is firstly introduced to detect a block of differential MPSK symbols over additive white Gaussian noise (AWGN) channel [9]. Applying MSDD to differential UWB-IR systems is considered in [10]–[12] firstly. Works [12], [13] consider the application of sphere decoding algorithm to fulfill a low complexity MSDD for differential UWB-IR systems. With the same purpose, work [12] proposed a Viterbi algorithm based MSDD and works [14]–[16] proposed decision-feedback MSDD.

Wireless communication systems are susceptible to various impairments, such as noises, interferences and channel fading. We usually employ channel codes to protect the transmitted symbols over possible errors. The decoding of most powerful channel codes that can approach the Shannon capacity depends on iterative algorithm, where iterations are performed between soft-in soft-out (SISO) modules [17]. These MSDD schemes mentioned earlier, however, are all about to detect the hard decisions of the differential modulated UWB-IR signals, which is not compatible with SISO channel decoding. Recently, the work [18] investigates SISO MSDD for UWB-IR systems and incorporate it with SISO channel decoding.

In this paper, we propose a new SISO MSDD scheme for noncoherent differential UWB-IR systems. Even without considering channel encoding, there are memories introduced by differential modulation to all modulated symbols throughout the transmitted packet. In [18], the SISO MSDD processes signal samples block-by-block and it just ignores the information dependencies among different blocks. This leads to information loss. In this paper, by contrast, the proposed SISO MSDD scheme calculates the soft information of one symbol by exploiting the signal samples from the whole packet. We propose an AcR architecture to enable this scheme. The proposed AcR architecture correlates the received UWB-IR

T. Wang is with Shenzhen University, China, and The Chinese University of Hong Kong, Hong Kong (email: wtt011@ie.cuhk.edu.hk).

T. Lv is with the School of Information and Communication Engineering, Beijing University of Posts and Telecommunications, China (email: lvtiejun@bupt.edu.cn).

H. Gao is with Singapore University of Technology and Design, Singapore (email: hui_gao@sutd.edu.sg).

S. Zhang is with Shenzhen University, China (email: zsl@szu.edu.cn).

T. Wang is supported by the Hong Kong PhD Fellowship Scheme. T. Lv is supported by the National Natural Science Foundation of China (NSFC) (Grant No. 61271188) and the China 973 Program (No. 2011CB302702).

signals, and dose not need explicit channel estimation. Thus, it is a noncoherent detection. Moreover, it can exploit the signal dependencies among the whole packet. We use a trellis graph to describe the statistical model of signal samples. We derive the SISO MSDD scheme using the belief propagation (BP) message passing which implements sum-product rule on a factor graph [19]. The proposed MSDD scheme is termed as BP-MSDD. We also consider SISO channel decoding. The outputs of the BP-MSDD are fed to the inputs of the BP algorithm for SISO channel decoding, and vice versa, in an iterative manner. The main contributions of this paper are summarized as the follows.

- 1) *New AcR architecture for SISO MSDD scheme.* We propose a new AcR architecture to sample the received UWB-IR signal. The AcR architecture results in a trellis statistical model for the signal samples of the whole transmitted packet. Compared with existing method, the proposed AcR can exploit more signal dependencies imposed by the differential modulation. This also enables us can apply BP message passing approach to noncoherent UWB-IR systems.
- 2) *Message passing approach for joint noncoherent detection and channel decoding scheme.* We apply BP message passing to the trellis-type signal model for deriving SISO MSDD scheme. The proposed BP-MSDD scheme is a bidirectional algorithm that consists of a forward and a backward message passing. Since BP message passing is employed as the decoding algorithm for many channel codes, we integrate the proposed BP-MSDD with BP algorithm for SISO channel decoding, and we achieve a iterative algorithm for the joint noncoherent detection and channel decoding scheme. We think this is the first time that applies BP message passing to noncoherent UWB-IR systems.
- 3) *Performance evaluations by simulations.* Simulations are performed to validate and evaluate the proposed scheme. The performances of uncoded and coded system under the environments of UWB multipath channel are evaluated. The results indicate the performance advantage of the proposed scheme over other existing schemes.

The rest of this paper is organized as follows. The system model of differential UWB-IR system is described in Section II. Section III introduces the joint noncoherent detection and channel decoding scheme. Section IV is about the parameter estimation in our system. Section V shows simulation results. Finally, conclusions are drawn in Section V.

II. SYSTEM MODEL

In this section, we establish the system model for UWB-IR communications. A block schematic diagram of the system model is shown in Fig. 1. Adopting binary antipodal pulse amplitude modulation (BPAM), the transmitted signal waveform is given by

$$s(t) = \sum_{i=0}^N d_i \omega_s(t - iT_s), \quad (1)$$

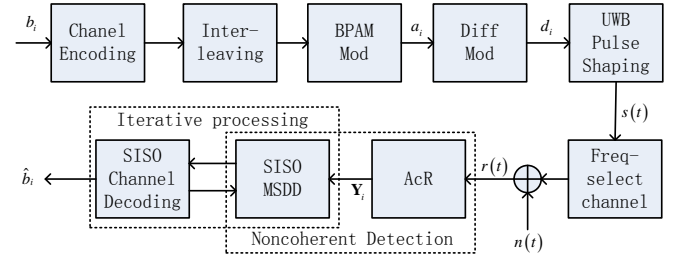


Fig. 1. A block schematic diagram of the system model.

where $d_i \in \{\pm 1\}$ is the channel symbol, $\omega_s(t)$ is the symbol waveform with duration T_s and N is the packet size. We denote the original information bits by $b_i \in \{0, 1\}$, $i = 1, \dots, K$. Through channel encoding, interleaving and modulation, these information bits are mapped to the coded data symbols $a_i \in \{\pm 1\}$, $i = 1, \dots, N$. The coding rate is $R = K/N$. Finally, the channel symbol d_i is obtained by differential modulation: $d_i = d_{i-1}a_i$, $i = 1, \dots, N$, where $d_0 = 1$ is the reference symbol. UWB-IR transmissions usually employ N_f frames to transmit one channel symbol, and each frame includes one very short pulse. According to this unique aspect of UWB-IR, the unmodulated symbol waveform used in (1) is expressed as

$$\omega_s(t) = \sum_{j=0}^{N_f-1} \omega(t - jT_f - c_jT_c), \quad (2)$$

where $\omega(t)$ is the ultra-short pulse with the duration T_ω (referred to as the monocycle in literatures), T_f is the frame duration and we have $T_s = N_fT_f$. The sequence $\{c_j\}$ in (2) is a user specific time-hopping (TH) code used for the purpose of multiple access. Its elements are integers in the range $0 \leq c_j \leq N_c - 1$, satisfying $T_f \geq N_cT_c$. T_c is the duration of an addressable time chip. Since $\omega(t)$ has a very short duration, T_ω is typically on the order of nanoseconds, the transmitted signal occupies a huge bandwidth. The frame duration T_f is usually hundred or thousand times longer than T_ω , resulting in a low duty transmission.

We consider dense multi-path environments, such as the industrial and indoor office [20]. The channel impulse response (CIR) between the transmitter and the receiver is modeled as $h(t) = \sum_{l=0}^{L-1} \alpha_l \delta(t - \tau_l)$, where δ is the Dirac delta function, L is the number of resolvable multipath components (MPCs), α_l and τ_l is the gain and the delay of the l^{th} MPC, respectively.

We define the received pulse waveform as: $g(t) \triangleq \omega(t) \otimes h(t)$, where \otimes denotes the convolution operator. Then, the received noisy signal waveform is given by

$$r(t) = s(t) \otimes h(t) + n(t) = \sum_{i=0}^N d_i \sum_{j=0}^{N_f-1} g(t - iT_s - jT_f - c_jT_c) + n(t), \quad (3)$$

where $n(t)$ is the additive white Gaussian noise process with zero mean and a flat two-sided power spectral density $N_0/2$. With T_g denoting the maximum delay spread of the received pulse waveform $g(t)$, the inter-frame interference (IFI) is avoided in the received signal (3) by letting $T_f > T_g + (N_c - 1)T_c$.

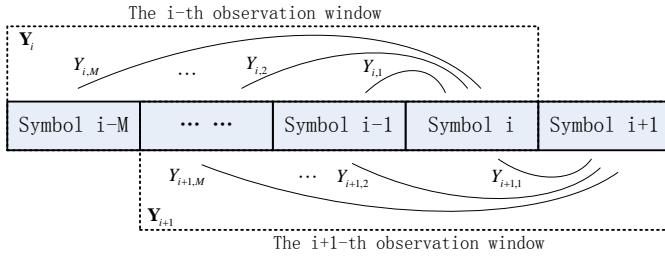


Fig. 2. The illustration for the sampling mechanism of the proposed AcR.

III. JOINT NONCOHERENT DETECTION AND CHANNEL DECODING

A. The Noncoherent Autocorrelation Receiver

The optimal coherent detection of UWB-IR signals requires a implementation of the filter matched to the received pulse waveform $g(t)$. However, the complexities of the implementation of match filtering and the explicit channel estimation constitute obstacles for the practical use of coherent detection in UWB-IR systems. Therefore, we focus on noncoherent detection that dose not involve the explicit channel estimation and the implementation of match filtering. To improve the performance of noncoherent detection, we apply the MSDD scheme to the system. UWB channels are quasi-static in typical indoor environments [20]. This means the channel remains invariant over several symbol durations. Relying on this feature, MSDD jointly detects a block of M symbols from the received signal in the observation window of size $M + 1$ symbol durations [10], [12], [18].

In this section, based on the concept of MSDD, we develop an AcR architecture for noncoherent detection of UWB-IR signals. We modify the sampling mechanism of the MSDD in [10], [12], [18]. Essentially, we still employ the correlation principle derived from GLRT criteria in [12] to sample the received signal; however, we change its sliding mode of the observation window. In [12], each time, the observation window of size $M + 1$ will be slid down M symbol durations after the current M symbols have been detected. In a different mode, we slide the $M + 1$ size observation window down one symbol duration each time. The sampling mechanism of the proposed AcR is illustrated in Fig. 2. In the following, we mathematically formulate the proposed sampling mechanism, and then explain its implications to noncoherent UWB-IR systems.

From the received signal $r(t)$ in the i^{th} observation window $(i - M)T_s \leq t \leq (i + 1)T_s$, we obtain the i^{th} sample vector $\mathbf{Y}_i \triangleq [Y_{i,1}, Y_{i,2}, \dots, Y_{i,M}]^T$, where $Y_{i,m}$ is the correlation sample between the i^{th} and the $(i - m)^{th}$ symbols

$$Y_{i,m} = \int_0^{T_g} y(t + iT_s)y(t + (i - m)T_s) dt \quad (4)$$

with the de-spreading signal

$$y(t) = \sum_{j=0}^{N_f-1} r(t + jT_f + c_jT_c). \quad (5)$$

After we finish the computation of \mathbf{Y}_i , the observation window is slid down one symbol duration to $(i + 1 - M)T_s \leq t \leq$

$(i + 2)T_s$, from where we will compute the next sample vector \mathbf{Y}_{i+1} . Since there is no transmission occurring ($r(t) = 0$ for $t < 0$), we pad some zeros at the rears of the first $M - 1$ sample vectors: $Y_{i,m} = 0$ for $i = 1, \dots, M - 1$ and $m = i + 1, \dots, M$. We make some remarks about the proposed AcR to bring out its implication.

- 1) The sampling mechanism of the proposed AcR also appears in [15], [16], where it is introduced by the concept of decision-feedback (DF). The DF based MSDD produces the correlations between the current symbol and the previous $M - 1$ symbols in the same way as (4); then it detects the current symbol by accepting the hard decisions of the previous $M - 1$ symbols as correct. As the hard decision about the current symbol is made, DF MSDD slides the observation window down one symbol duration to detect the next symbol. It is different from [15], [16] that we will employ the proposed AcR to fulfill SISO MSDD rather than hard decision.
- 2) Based on the samples of the whole packet \mathbf{Y}_i for $i = 1, \dots, N$ produced by the proposed AcR, we will derive the BP message passing algorithm for SISO MSDD in the next subsection. The idea is to build up a trellis graph model for the whole packet of samples. The BP message passing algorithm performs statistic inference about the data symbols by propagating their certainties throughout the trellis graph. We also incorporate the message passing algorithm for channel decoding, which results in a message passing framework for joint noncoherent detection and channel decoding in UWB-IR systems.
- 3) The sampling mechanism of [10], [12], [18] is on a block-by-block basis. The correlation operations try to exploit the dependencies (imposed by the differential modulation) among symbols within a block of M symbols. However, the symbol dependencies between different blocks are ignored. This is a kind of information loss. Depending upon the proposed sampling mechanism where blocks overlap some others, the detection of one symbol is able to make use of the information of all the symbols throughout the packet. Since more information are collected, it is expected that the proposed scheme could have better performance.

B. The BP Message Passing Algorithm for SISO MSDD

In what follows, we derive the BP message passing algorithm for SISO MSDD using the samples delivered from the proposed AcR. Substituting (5), (3) into (4) and using the result of differential demodulation $d_i d_{i-m} = \prod_{z=m+1}^i a_z$, we can express the sample $Y_{i,m}$ as

$$Y_{i,m} = \left(\prod_{z=m+1}^i a_z \right) N_f^2 E_g + n_{i,m}, \quad (6)$$

where $E_g \triangleq \int_0^{T_g} g^2(t) dt$ is the captured energy of the received pulse and $n_{i,m}$ is the discrete noise component. It has been shown in [21] that $Y_{i,m}$ for all i and m can be approximated to mutually independent Gaussian random variables with mean $\left(\prod_{z=m+1}^i a_z \right) N_f^2 E_g$ and variance $\sigma_n^2 =$

$N_f N_0 E_g + W T_g N_0^2 / 2$, where W is the bandwidth of the bandpass filter employed by the receiver. This approximation is rather well when N_f is large due to central limit theorem. It can be concluded from (6) that the signal samples depends on the data symbols and the captured energy E_g . To obtain the knowledge of parameter E_g , our receiver employs an energy estimation method: $\hat{E}_g = \sqrt{\sum_{i,m} Y_{i,m}^2 / (Z N_f^4)}$, where Z is the number of non-zero elements in $\{\mathbf{Y}_i\}$. Then, we detect data symbols by just assuming the perfect knowledge of E_g . In the simulation results of Section IV, we will see that this straightforward estimation of E_g achieves a rather good performance.

Let $\mathbf{Y} \triangleq \{\mathbf{Y}_i\}$ be the set containing all the sample vectors and $\mathbf{a} \triangleq [a_1, a_2, \dots, a_N]^T$ be the vector of all the data symbols. The constraint on \mathbf{a} by channel encoding will be discussed in the next subsection, and we ignore it here. The target of the BP-MSDD is to calculate the a posteriori probability (APP) of data symbol a_i given \mathbf{Y} :

$$p(a_i | \mathbf{Y}) \propto \sum_{\mathbf{a}: \sim a_i} p(\mathbf{Y} | \mathbf{a}) p(\mathbf{a}) \quad (7)$$

for all i , where the notation $\sum_{\mathbf{a}: \sim a_i}$ means summation over all data symbols in \mathbf{a} except a_i . The straightforward calculation of (7) will involve complexity $O(2^N)$, which disastrously increases with N . We will develop the trellis representation for the system and employ BP message passing to it for an efficient calculation of (7). To derive the BP message passing, we need to factorize the globe probability function $p(\mathbf{Y} | \mathbf{a}) p(\mathbf{a})$ into many small local functions and model the system using a factor graph. Specified by (6), we meet an equivalent discrete memory channel. The i^{th} sample vector \mathbf{Y}_i is a function of the M coded data symbols a_{i-m} for $m = 0, 1, \dots, M-1$. Therefore, we can factorize $p(\mathbf{Y} | \mathbf{a})$ as

$$p(\mathbf{Y} | \mathbf{a}) = \prod_{i=1}^N p(\mathbf{Y}_i | a_i, a_{i-1}, \dots, a_{i-M+1}), \quad (8)$$

where

$$p(\mathbf{Y}_i | a_i, a_{i-1}, \dots, a_{i-M+1}, E_g) \propto \prod_{m=1}^M \exp \left(- \left| Y_{i,m} - \left(\prod_{z=m+1}^i a_z \right) N_f^2 E_g \right|^2 / \sigma_n^2 \right). \quad (9)$$

is obtained by using the Gaussian approximation of $Y_{i,m}$ given a_{i-m} for $m = 0, 1, \dots, M-1$. Then, we perform a trivial factorization on $p(\mathbf{a})$:

$$\begin{aligned} p(\mathbf{a}) &= \prod_{i=1}^N p(a_i) \\ &= \prod_{i=1}^N p(a_i, a_{i-1}, \dots, a_{i-M+1} | a_{i-1}, a_{i-2}, \dots, a_{i-M}) \end{aligned} \quad (10)$$

which, however, will be useful to bring out the trellis representation of the system.

We now define a trellis to model the discrete memory channel represented by (8) as follows. The i^{th} state is $\mathbf{S}_i \triangleq [a_i, a_{i-1}, \dots, a_{i-M+1}]^T$. The i^{th} input is a_i . The i^{th} output is $\mathbf{x}_i \triangleq [a_i, a_{i-1}, \dots, a_{i-M+1}]^T$. The local

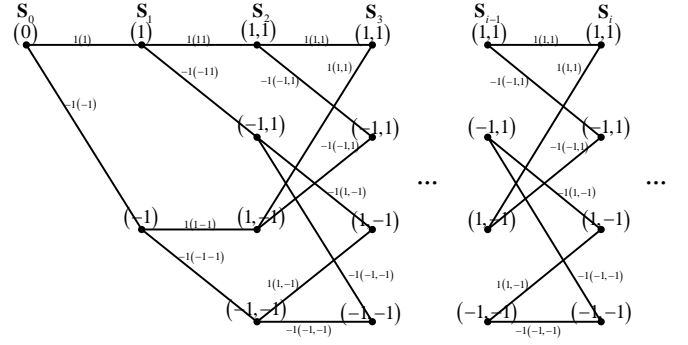


Fig. 4. An example of the defined trellis with $M = 2$. The digits one each transition represent the associated input(outputs): $a_i(\mathbf{x}_i)$.

check function for the transition from state $i-1$ to state i on the trellis is $T_i(a_i, \mathbf{x}_i, \mathbf{S}_{i-1}, \mathbf{S}_i)$: $T_i = 1$ when the combinations of its arguments are possible; $T_i = 0$ otherwise. An example of this trellis with $M = 2$ is given in Fig. 3. This trellis definition is also consistent with the factorization in (10): $T_i(a_i, \mathbf{x}_i, \mathbf{S}_{i-1}, \mathbf{S}_i) \propto p(a_i, a_{i-1}, \dots, a_{i-M+1} | a_{i-1}, a_{i-2}, \dots, a_{i-M})$. Therefore, we have

$$p(\mathbf{a}) \propto \prod_{i=1}^N T_i(a_i, \mathbf{x}_i, \mathbf{S}_{i-1}, \mathbf{S}_i). \quad (11)$$

Substituting (8), (11) into (7) leads to

$$\begin{aligned} p(a_i | \mathbf{Y}) &\propto \underbrace{\left(\sum_{\mathbf{a}_{1:i-1}} \prod_{j=1}^{i-1} p(\mathbf{Y}_j | \mathbf{x}_j) T_j(a_j, \mathbf{x}_j, \mathbf{S}_{j-1}, \mathbf{S}_j) \right)}_{\triangleq \alpha(\mathbf{S}_{i-1})} \\ &\times \underbrace{\left(\sum_{\mathbf{a}_{i+1:N}} \prod_{j=i+1}^N p(\mathbf{Y}_j | \mathbf{x}_j) T_j(a_j, \mathbf{x}_j, \mathbf{S}_{j-1}, \mathbf{S}_j) \right)}_{\triangleq \beta(\mathbf{S}_i)} \\ &\times p(\mathbf{Y}_i | \mathbf{x}_i) T_i(a_i, \mathbf{x}_i, \mathbf{S}_{i-1}, \mathbf{S}_i) \end{aligned} \quad (12)$$

Based on the expression (12), we can now calculate $p(a_i | \mathbf{Y})$ using the BP message passing algorithm that implements the sum-product principal [19]. To visualize the BP message passing for SISO MSDD, we employ a factor graph to model the system. The factor graph of the system is shown in Fig. 4, where circles are variable nodes for inputs and outputs, double circles are variable nodes for state and squares are the factor nodes for check functions.

The resultant BP message passing algorithm consists of a forward and backward message passing, which is similar to the BCJR algorithm [22]. The forward message passing recursively calculates the message $\alpha(\mathbf{S}_i)$ which is already defined in (12):

$$\alpha(\mathbf{S}_i) \propto \sum_{\mathbf{S}_{i-1}} \alpha(\mathbf{S}_{i-1}) p(\mathbf{Y}_i | \mathbf{x}_i) T_i(a_i, \mathbf{x}_i, \mathbf{S}_{i-1}, \mathbf{S}_i) \quad (13)$$

for each $i = 1, 2, \dots, N$, where $T_i(a_i, \mathbf{x}_i, \mathbf{S}_{i-1}, \mathbf{S}_i)$ is the previously defined local check function for the trellis transition,

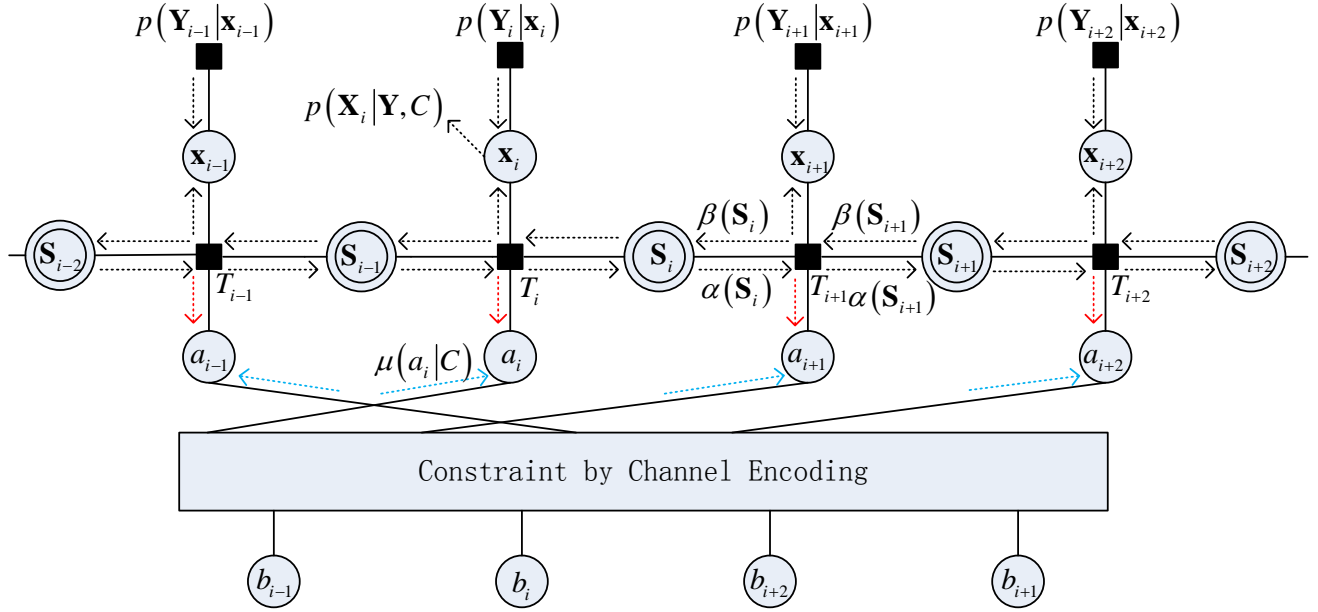


Fig. 3. The factor graph for joint noncoherent detection and channel decoding, where the red arrows denote the intrinsic information sent from the BP-MSDD to the BP channel decoding and the blue arrows denote the intrinsic information sent from the BP channel decoding to the BP-MSDD.

and $p(\mathbf{Y}_i|\mathbf{x}_i)$ is the information from observation \mathbf{Y}_i (shown in (9)). Similarly, the backward message passing recursively calculates the message $\beta(\mathbf{S}_i)$ which is already defined in (12):

$$\beta(\mathbf{S}_i) \propto \sum_{\mathbf{S}_{i+1}} \beta(\mathbf{S}_{i+1}) p(\mathbf{Y}_{i+1}|\mathbf{x}_{i+1}) T_{i+1}(a_{i+1}, \mathbf{x}_{i+1}, \mathbf{S}_i, \mathbf{S}_{i+1}) \quad (14)$$

for each $i = 1, 2, \dots, N$. After the forward and backward message passing once in each direction, the APPs of a_i for each $i = 1, 2, \dots, N$ are given by

$$p(a_i|\mathbf{Y}) \propto \sum_{\mathbf{a}_i} \alpha(\mathbf{S}_{i-1}) \beta(\mathbf{S}_i) p(\mathbf{Y}_i|\mathbf{x}_i) p(a_i) T_i(a_i, \mathbf{x}_i, \mathbf{S}_{i-1}, \mathbf{S}_i), \quad (15)$$

where $p(a_i)$ is the priori information of a_i , which is a constant. We now finish the derivations on the BP-MSDD scheme.

C. Joint Noncoherent Detection and Channel Decoding

BP message passing algorithm is also widely used as the decoding algorithm for many advanced channel codes, such as LDPC code, Turbo code and RA code [17], [19]. It is straightforward to integrate BP-MSDD with BP channel decoding under the message passing framework, resulting in a BP message passing algorithm for joint noncoherent detection and channel decoding. In this section, we consider channel encoding part. We denote the valid set of codeword by C , and all related probability functions should be conditioned on C hereafter. The factor graph of the overall system includes channel encoding constraint is shown in Fig. 4.

The presence of the constraint on a by channel encoding introduces loops onto the factor graph. As a consequence, the BP message passing cannot exactly calculate these APPs of interest, and it is an iterative algorithm: the message will be passed multiple times on some given edges of the factor graph

[19]. Fortunately, in many applications, the approximation of APPs by iterative BP message passing is pretty good.

Given the considered factor graph, we can design many different message-passing schedules. In this work, we adopt a serial schedule [19] for iterative BP message passing between the BP-MSDD and channel decoder. The messages exchanged between the BP-MSDD and channel decoder are known as the extrinsic information. In particular, given the messages from observations \mathbf{Y} and the extrinsic information from channel decoding, the BP-MSDD performs the message passing algorithm derived in Section III.B to calculate the APPs of all a_i : the computation is still according to (15) with the only difference that we replace the priori information a_i with the intrinsic information of a_i sent the from channel decoder. These APPs of a_i are treated as extrinsic information (denoted by red arrows in Fig. 4) which will be delivered to channel decoder. Then, given these extrinsic information from the BP-MSDD, the channel decoder runs several rounds of BP message passing within the subgraph of channel encoding constraint. After that, the channel decoder sends back its extrinsic information (denoted by blue arrows in Fig. 4) to the BP-MSDD for the next iteration. After K_{BP} iterations between the BP-MSDD and channel decoder, we terminate the algorithm, and obtain the final decoding results about information bits.

Finally, we remark that the above iterative processing is implemented in digital domain as long as we have obtained the correlation samples from the AcR receiver, which can be realized using analog components to avoid the ultra high sampling rate in UWB-IR systems. A block schematic diagram about this receiver structure is also shown in Fig. 1.

IV. NUMERICAL RESULTS

In this section, simulations are conducted to validate the proposed scheme. In all simulations, the channel are generated according to IEEE 802.15.3a CM2 model [23], and the channel impulse responses are truncated at $T_g = 100$ ns. The used impulse shape $\omega(t)$ is the second derivative of a Gaussian function. The duration of $\omega(t)$ is set as $T_w = 0.5$ ns. The frame and chip duration are set to $T_f = 200$ ns and $T_c = 1.0$ ns, respectively. Each symbol consists of $N_f = 10$ frames. The TH codes are randomly picked up in the interval $[0, N_c - 1]$ where $N_c = 100$. Since now $T_f > T_g + (N_c - 1)T_c$ is satisfied, there is no IFI in our system. The integration interval of AcR is $T_i = T_g = 100$ ns. The bandwidth of the baseband filter employed at the receiver is 2 GHz. The energy used to transmit one information bit is denoted by E_b , and the signal-to-noise ratio (SNR) is defined as E_b/N_0 .

A. The performance of uncoded system

We first investigate the performance of the proposed BP-MSDD scheme for uncoded differential UWB-IR systems. Without considering channel codes, we employ the BP-MSDD to detect the data symbols a_i for $i = 1, 2, \dots, N$. After the bidirectional message passing, the BP algorithm outputs the APP of a_i as in (15). Then, the hard decision about a_i is made based upon (15). Each packet consists of $N = 1024$ data symbols. We evaluate the BER performance of the proposed BP-MSDD scheme with perfect E_g and estimated E_g . As benchmarks, we also evaluate the BER performances of the DD [7] scheme and MSDD [10], [12] scheme for differential UWB-IR systems.

Fig. 5 presents the simulation results. The first point we want to study is the impact of E_g on the system performance. We can observe from Fig. 5 that the BP-MSDD schemes with perfect E_g and estimated E_g nearly have the same performance. Thus, we can conclude that the estimate of E_g by the simple energy estimation method is sufficiently effective for the implementation of BP-MSDD. Then, compared with DD scheme, the proposed BP-MSDD scheme can further improve the uncoded performance by offering an additional detection gain which increases with M . This performance trend of BP-MSDD is similar to that of MSDD. Moreover, we see that BP-MSDD has a better performance than MSDD, e. g. 0.7 dB gain with $M = 2$ and 1dB gain with $M = 5$ at the BER of 10^{-5} .

B. The performance of coded system

We then investigate the performance of the proposed joint BP-MSDD and channel decoding for coded differential UWB-IR systems. The regular RA code [24] with coding rate 1/3 is employed. Each packet has 1024 information bits (thus 3072 channel-coded data symbols). The energy estimation method is used to obtain the estimate of E_g . The performances of the joint MSDD and channel decoding proposed in [18] will be presented as the benchmarks. For all simulation results, we perform 8 iterations between the BP-MSDD and the BP for RA channel decoding, and 20 iterations within the RA channel decoder.

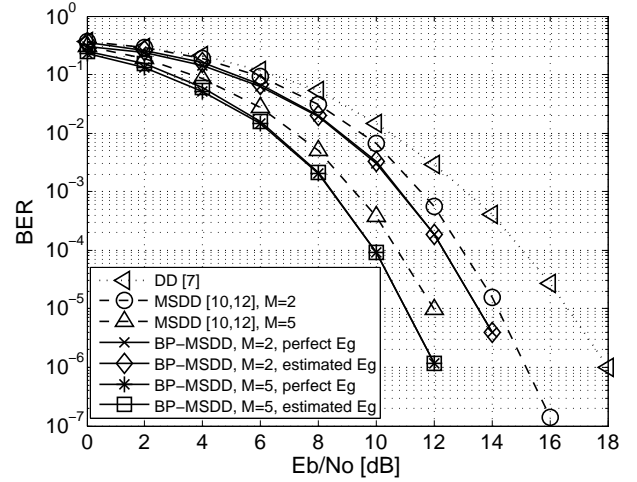


Fig. 5. The BER results of the uncoded system.

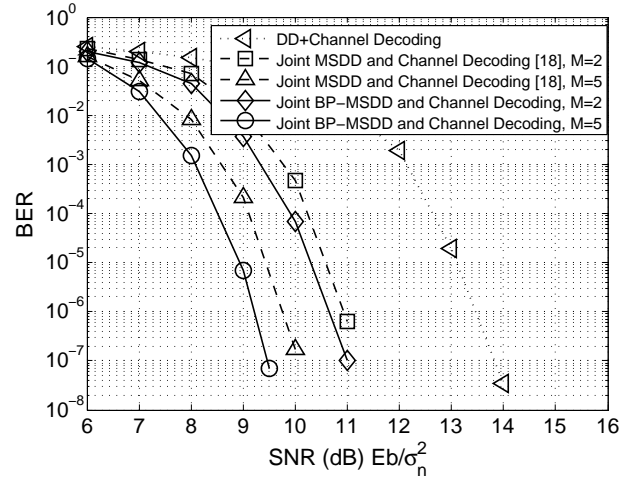


Fig. 6. The BER results of the coded system.

Fig. 6 presents the simulation results. We can see that the proposed joint BP-MSDD and channel decoding scheme has a better performance than the joint MSDD and channel decoding scheme. And, the gain is increased with M , e. g. 0.3 dB gain with $M = 2$ and 0.6 dB gain with $M = 5$ at the BER of 10^{-6} . We believe that these gains are due to the more beliefs collected by the BP message passing for BP-MSDD.

V. CONCLUSION

In this paper, we apply BP algorithm to propose a joint non-coherent detection and channel decoding scheme for UWB-IR systems. Specifically, we propose a new AcR architecture to transform the received UWB-IR signal into discrete samples, whose statistical model has a trellis structure. Using this trellis model and BP algorithm, we derive a new SISO MSDD for computing the APPs of the data symbols. The proposed BP-MSDD is a bidirectional message passing algorithm, which can makes use of all the signal dependences throughout the whole packet. Thus, it has better performance than the block independent MSDD. Then, we feed the outputs of BP-MSDD to the inputs of BP channel decoding, and vice versa, in an

iterative manner. Simulations illustrate the superiority of the proposed scheme over other existing schemes.

- [24] D. Divsalar, H. Jin, and R. J. McEliece, "Coding theorems for turbo-like codes," in *Proc. 36th Annual Allerton Conf. on Communication, Control and Computing*, Allerton, Monticello, IL, Sept. 1998, pp. 201–210.

REFERENCES

- [1] L. Yang and G. Giannakis, "Ultra-wideband communications: an idea whose time has come," *IEEE Signal Process. Mag.*, vol. 21, no. 6, pp. 26–54, Jun. 2004.
- [2] A. Rajeswaran, V. S. Somayazulu, and J. R. Foerster, "Rake performance for a pulse based UWB system in a realistic UWB indoor channel," in *Proc. 2003 IEEE Int. Conf. Commun.*, 2003, pp. 2879–2883.
- [3] M. Win and R. Scholtz, "On the energy capture of ultrawide bandwidth signals in dense multipath environments," *IEEE Commun. Lett.*, vol. 2, no. 9, pp. 245–247, Sep. 1998.
- [4] V. Lottici, A. D'Andrea, and U. Mengali, "Channel estimation for ultra-wideband communications," *IEEE J. Sel. Areas Commun.*, vol. 20, no. 9, pp. 1638–1645, Sep. 2002.
- [5] J. Chen, T. Lv, Y. Chen, and J. Lv, "A timing-jitter robust uwb modulation scheme," *IEEE Signal Process. Lett.*, vol. 13, no. 10, pp. 593–596, 2006.
- [6] K. Witrisal, G. Leus, G. Janssen, M. Pausini, F. Troesch, T. Zasowski, and J. Romme, "Noncoherent ultra-wideband systems," *IEEE Signal Process. Mag.*, vol. 26, no. 4, pp. 48–66, Apr. 2009.
- [7] M. Ho, V. Somayazulu, J. Foerster, and S. Roy, "A differential detector for an ultra-wideband communications system," in *Proc. IEEE 55th Vehicular Technology Conference*, May 2002, pp. 1896–1900.
- [8] J. Choi and W. Stark, "Performance of ultra-wideband communications with suboptimal receivers in multipath channels," *IEEE J. Sel. Areas Commun.*, vol. 20, no. 9, pp. 1754–1766, Sep. 2002.
- [9] D. Divsalar and M. Simon, "Multiple-symbol differential detection of MPSK," *IEEE Trans. Commun.*, vol. 38, no. 3, pp. 300–308, Mar. 1990.
- [10] N. Guo and R. Qiu, "Improved autocorrelation demodulation receivers based on multiple-symbol detection for UWB communications," *IEEE Trans. Wireless Commun.*, vol. 5, no. 8, pp. 2026–2031, Aug. 2006.
- [11] Y. Tian and C. Yang, "Noncoherent multiple-symbol detection in coded ultra-wideband communications," *IEEE Trans. Wireless Commun.*, vol. 7, no. 6, pp. 2202–2211, Jun. 2008.
- [12] V. Lottici and Z. Tian, "Multiple symbol differential detection for UWB communications," *IEEE Trans. Wireless Commun.*, vol. 7, no. 5, pp. 1656–1666, May 2008.
- [13] T. Wang, T. Lv, and H. Gao, "Sphere decoding based multiple symbol detection for differential space-time block coded ultra-wideband systems," *IEEE Commun. Lett.*, vol. 15, no. 3, pp. 269–271, Mar. 2011.
- [14] Q. Zhou, X. Ma, and V. Lottici, "Fast multi-symbol based iterative detectors for UWB communications," *EURASIP Journal on Advances in Signal Processing*, vol. 2010, pp. 1–14, May 2010.
- [15] A. Schenk and R. Fischer, "Decision-feedback differential detection in impulse-radio ultra-wideband systems," *IEEE Trans. Commun.*, vol. 59, no. 6, pp. 1604–1611, Jun. 2011.
- [16] T. Wang, T. Lv, H. Gao, and Y. Lu, "BER analysis of decision-feedback multiple-symbol detection in noncoherent MIMO ultrawideband systems," *IEEE Trans. Veh. Technol.*, vol. 62, no. 9, pp. 4684 – 4690, Nov. 2013.
- [17] N. Wiberg, H.-A. Loeliger, and R. Kotter, "Codes and iterative decoding on general graphs," *European Trans. Telecommun.*, vol. 6, no. 5, pp. 513–525, 1995.
- [18] Q. Zhou and X. Ma, "Soft-input soft-output multiple symbol differential detection for uwb communications," *IEEE Commun. Lett.*, vol. 16, no. 8, pp. 1296–1299, 2012.
- [19] F. R. Kschischang, B. J. Frey, and H.-A. Loeliger, "Factor graphs and the sum-product algorithm," *IEEE Trans. Inf. Theory*, vol. 47, no. 2, pp. 498–519, 2001.
- [20] A. Molisch, D. Cassioli, C. Chong, S. Emami, A. Fort, B. Kannan, J. Karedal, J. Kunisch, H. Schantz, K. Siwiak *et al.*, "A comprehensive standardized model for ultrawideband propagation channels," *IEEE Trans. Antennas Propag.*, vol. 54, no. 11, p. 3151, November 2006.
- [21] T. Quek and M. Win, "Analysis of UWB transmitted-reference communication systems in dense multipath channels," *IEEE J. Sel. Areas Commun.*, vol. 23, no. 9, pp. 1863–1874, Sep. 2005.
- [22] L. Bahl, J. Cocke, F. Jelinek, and J. Raviv, "Optimal decoding of linear codes for minimizing symbol error rate," *IEEE Trans. Inf. Theory*, vol. 20, no. 2, pp. 284–287, 1974.
- [23] J. Foerster, "Channel Modeling Subcommittee Report Final (doc.: IEEE802-15-02/490rl-SG3a). IEEE P802. 15 Working Group for Wireless Personal Area Networks (WPANs), Feb. 2002."